HORIZONTAL SHEAR CAPACITY OF COMPOSITE CONCRETE BEAMS WITHOUT TIES

Dean Deschenes[1], ATLSS Research Center, Lehigh University, Bethlehem, PA
Clay Naito[2], ATLSS Research Center, Lehigh University, Bethlehem, PA

ABSTRACT

To ensure composite action between precast concrete bridge beams and cast-in-place decks, horizontal shear ties are used. The shear ties prevent relative slip between the concrete elements; thereby maintaining monolithic behavior after the initial concrete interface shear capacity is lost. Current requirements for horizontal shear are conservative and only allow for a nominal amount of concrete-to-concrete shear capacity. This results in an uneconomical amount of steel crossing the composite interface. To examine the viability of increasing the allowable concrete horizontal shear capacity, structural testing of composite prestressed beams without horizontal shear ties was conducted. The horizontal shear capacity was established for uniform and point load conditions, four levels of interface roughness, and three ratios of slab to beam concrete compressive strength. Horizontal shear interface design recommendations are presented and compared to current design codes. The recommendations suggest that the interface bond capacity is greater than capacities currently prescribed by AASHTO LRFD and ACI 318.

Keywords: Horizontal, Shear, Ties, Prestressed, Composite, Concrete

[1] (Presenting Author) Research Assistant. ATLSS Research Center, Lehigh University, 117 ATLSS Dr., Bethlehem, PA, 18015, Email: djd2@lehigh.edu

[2] Assistant Professor of Structural Engineering. Lehigh University, 117 ATLSS Dr., Bethlehem, PA, 18015, Email: cjn3@lehigh.edu

INTRODUCTION

Precast, prestressed concrete is a widely preferred material for the design and construction of bridge systems. The combination of quality precast elements and a cast-in-place deck results in accelerated construction, durability, and low maintenance. Further optimization of the system is achieved when beam and deck elements are designed to act compositely. Such construction allows the beam-slab section to act as a single unit, thereby maintaining monolithic efficiency, reducing beam sizes, and lowering material costs.

A composite bridge system is only possible if the beam-slab interface transfers all unbalanced forces, without slipping. These horizontal shear forces are transferred across the composite joint through a combination of interface cohesion and aggregate interlock. If the system loading exceeds the horizontal shear stress capacity, the bond is lost and slip initiates. Horizontal shear ties extending across the joint (if present) are then engaged to resist further slip and maintain integrity of the beam-slab system.

Historically, vertical reinforcement crossing the beam – slab interface has been considered to be the primary means for transferring shear between the interfaces. Other factors affecting the capacity, such as joint roughness and element concrete strength, have typically been considered to provide only limited contribution. Design approaches have consequently taken a similar approach. The ACI standard and AASHTO LRFD design code limit the horizontal shear resistance for an un-reinforced, roughened interface to 80 and 100 psi, respectively.[22,23] Although limited, early data obtained by Mattock and others suggests that the same un-reinforced, roughened interface could achieve up to 500 psi before breakdown.[6] This disparity between the design approach and research findings has been neglected for many years. The results and observations presented here hope to provide a fresh insight into the horizontal shear capacity of composite systems without ties.

HORIZONTAL SHEAR CAPACITY – DESIGN APPROACHES

When the first recommendations for composite construction were released by a joint ACI-ASCE committee in 1960, provisions for the capacity of bonds without ties were absent.[5] Although revisions have been made since, the conservative nature of the codified approaches still limits the horizontal shear capacity of topped systems without ties to very low levels. Current techniques used to calculate interface capacities are presented below.

American Concrete Institute (ACI 2005)

The design approach for horizontal shear in a composite concrete beam is outlined in Section §17.5 of the ACI 318-05 standard.[22] Addressing interface design in terms of forces, it specifies that the factored horizontal shear force capacity (φV_{nh}) must exceed the factored vertical shear force demand (V_u). Although the horizontal shear capacity is further defined for four different interface conditions, only one applies to the un-reinforced interface considered here. As stated in ACI Section §17.5.3.1, an interface that is "clean, free of laitance, and intentionally roughened" shall not have a capacity greater than:

$$\begin{array}{lll} \textit{Force}\ [\text{lbs}] & V_{nh} = 80 b_v d & \\ \textit{Stress}\ [\text{psi}] & v_{nh} = 80 & \text{(Eq. 1)} \end{array}$$

where,

b_v = width of beam-slab interface [in.]

d = the distance from extreme compression fiber to the centroid of longitudinal tension reinforcement [in.]

American Association of State Highway and Transportation Officials (LRFD 2006)

Like the ACI standard, AASHTO LRFD Section §5.8.4 addresses horizontal shear design in terms of forces at the interface.[23] The factored horizontal shear capacity (φV_n) must exceed the factored horizontal shear demand (V_h). In regards to an un-reinforced interface, AASHTO states that the horizontal shear capacity shall be taken as:

$$\begin{array}{lll} \textit{Force}\ [\text{lbs}] & V_n = c \cdot (b_v \cdot d\ell) + \mu \cdot P_c & \\ \textit{Stress}\ [\text{psi}] & \begin{array}{l} v_{nr} = 100 \\ v_{nu} = 75 \end{array} & \text{(Eq.2)} \end{array}$$

where,

v_{nr} = shear stress capacity for a clean, intentionally roughened interface roughened to an amplitude of 0.25 in. [psi]

v_{nu} = shear stress capacity for a clean, but not intentionally roughened interface free of laitance [psi]

c = cohesion factor [psi] = (100 for v_{nr}) or (75 for v_{nu})

A_{cv} = area of concrete engaged in shear transfer [in^2]

μ = friction factor for normal weight concrete = (1.0 for v_{nr}) or (0.6 for v_{nu})

P_c = permanent compressive force normal to the shear plane, usually neglected [lbs]

HORIZONTAL SHEAR DEMAND – ANALYSIS METHODS

Horizontal shear demand is computed using one of three general approaches: 1) global force equilibrium, 2) simplified elastic beam behavior, and 3) classical elastic methods. These methods can be summarized by examining a beam subject to uniform loading (Figure 1).

Global Force Equilibrium

Global force equilibrium equates the horizontal shear demand to the change in topping force from one section to another. In practice, the compression at two discrete points along the beam is computed. The difference between these compression forces is then divided by the contact area over which the force difference is transferred, resulting in the equivalent horizontal shear stress (v_h) at the interface (Eq.3 and Figure 1-A).

$$\textit{ACI \& AASHTO} \text{ [psi]} \qquad v_h = \left(C_1 - C_2\right)/(\ell \cdot b_v) \qquad \text{(Eq. 3)}$$

where,

v_h = Horizontal shear stress at interface [psi]
C_1 = Force in topping at point 1 [lbs]
C_2 = Force in topping at point 2 [lbs]
l = Interface length between points 1 and 2 [in.]

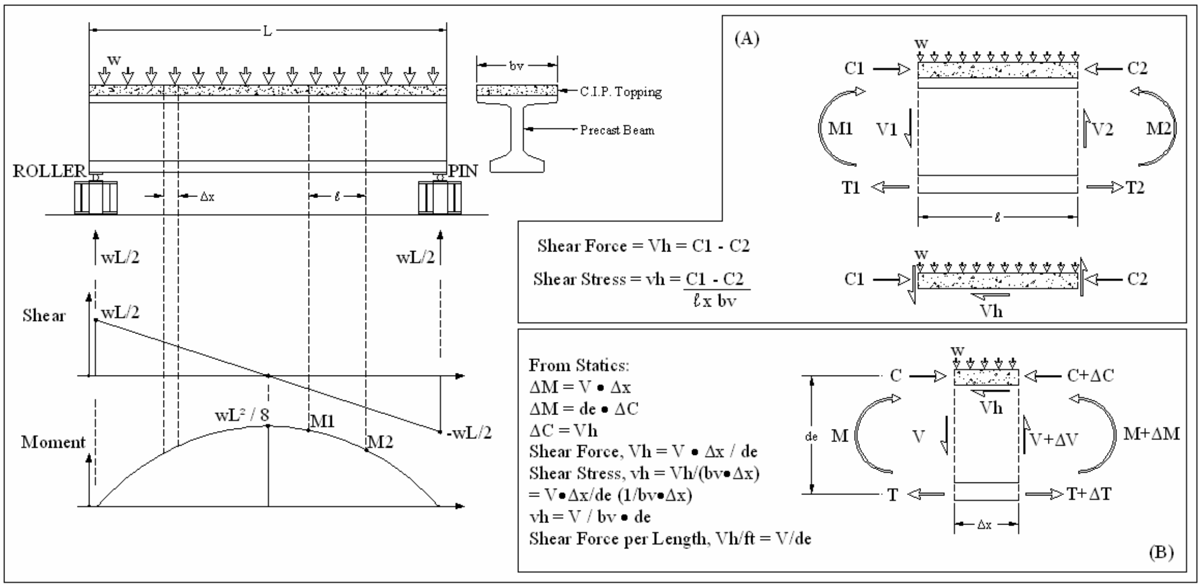

Figure 1: Horizontal shear demand calculation methods

Simplified Elastic Beam Behavior

The second method uses flexural beam theory to equate the horizontal shear demand to the vertical shear acting on the section. A small segment (Δx) of the beam is evaluated. From force equilibrium, a relationship between the vertical shear on the section and the horizontal shear stress can be determined. The derivation is summarized in Figure 1-B, with the final result noted as Equation 4,

$$\begin{aligned} &\textit{ACI} \text{ [psi]} && v_h = {}^{V}\!/_{b_v d} \\ &\textit{AASHTO} \text{ [psi]} && v_h = {}^{V}\!/_{b_v d_e} \end{aligned} \qquad \text{(Eq. 4)}$$

where,

V = Factored vertical shear force at the section [lbs]
d_e = Distance between the centroid of the tension reinforcement to the center of the compression zone [in.]

Classical Elastic Methods

A majority of previous horizontal shear studies have used the elastic method to determine both service and failure level horizontal shear stresses. Although the equation does not hold true at the ultimate strength level, the nonlinearities can be approximated using the cracked-section properties.[16] The elastic method is summarized in Equation 5.

$$v_h = \frac{VQ}{Ib_v} \qquad \text{(Eq. 5)}$$

where,

Q = First moment of inertia with respect to the neutral axis of the slab [in^3]
I = Moment of inertia of the entire composite cross-sectional area [in^4]

Although previous studies have shown that AASHTO Equation 4 and Equation 5 predict similar stresses at service levels, the classical method has the advantage of using cracked section properties for failure loads. The use of the technique will be compared to other methods and validated with experimental data later in this paper.

PREVIOUS RESEARCH

Previous research suggests that the horizontal shear capacity of an un-reinforced joint is much greater than the current, ACI (unchanged since 1971) and AASHTO allowances.[1,2,4,9-11,15,17,18] The failure to update these provisions can be attributed to the lack of results for un-reinforced composite systems. From 1976 to 1998, few if any composite beams without ties were tested. Relevant data prior to that period was extremely limited and did not include results for all of the factors affecting interface behavior (i.e. interface roughness, concrete strength, and reinforcement area). In 1999, Patnaik examined nine composite beams without interface reinforcement.[19] The study and the previous work by others confirms the conservative nature of the codified approaches (Table 1).

To date, horizontal shear demand analyses have not been validated for composite prestressed sections. Loov and Patnaik[16] compared the methods outlined above, but did not validate any particular technique with experimentally measured results. Although their study provided insight on how the equations compare with each other, it did not comment on the accuracy of the techniques (at both service and failure load levels). Furthermore, since the founding research was conducted during the late 1950s and early 1960s, high strength concrete has become readily available. A proper experimental study incorporating prestressed sections and higher strength concrete is needed to validate analytical methods used in practice.

Table 1: Previous research results[1,2,4,9-11,15,17-19]

Specimen ID	Concrete Strength [ksi]	Horizontal Shear Stress Capacity [psi]	Source
BR-I	3.18	400.30	Hanson
15C	3.03	390.15	Saemann and Washa
16C	3.03	601.91	Saemann and Washa
1	4.89	465.57	Evans and Chung
SG-2	2.39	311.83	Bryson and Carpenter
R0.0	3.74	565.65	Nosseir and Murtha
LRE-5	3.92	266.87	CTA-76-B4
RR1.1	2.87	227.71	Patnaik
RR1.2	2.87	262.52	Patnaik
RR2.1	3.41	272.67	Patnaik
RR2.2	3.41	269.77	Patnaik
RR3.1	2.47	252.37	Patnaik
RR3.2	2.47	258.17	Patnaik
RHR1	9.05	462.67	Patnaik
RHR2	9.05	427.86	Patnaik
RHR3	9.05	474.27	Patnaik
	Average	369.39	

EXPERIMENTAL PROGRAM

Research Variables

The experimental program investigates the horizontal shear capacity of prestressed concrete beams with cast-in-place reinforced concrete topping slabs. The interface roughness and topping slab compressive strength is varied to assess the different conditions that may exist in building and bridge construction.

a) As-Placed (A)	b) Broom (B)	c) ¼" Rake (R)	d) Sheepsfoot (Sh)

Figure 2: Interface finishes

The interface surface roughness was varied using five practical surfacing techniques typically conducted in precast operations: as-placed roughness, broom finish, ¼" rake finish, smooth finish, and sheepsfoot voids (see Figure 2). The as-placed condition represents the minimum level of work required by the precast producer. High slump (6-in.) concrete is placed with internal vibration and the surface is left unfinished. The broom and rake finishes were made using standard procedures, i.e., a broom or rake was run across the surface transverse to the beam length. The sheepsfoot represents a mechanical surface finish consisting of 1-in. diameter, ½-in. deep impressions made at a spacing of 3½-in. The interface was clean and free of laitance prior to the placement of the flange concrete.

The flange concrete compressive strength was varied to represent conditions typical of precast construction. The strength was varied from low to high. The measured compressive strengths included 3.11, 5.67, 8.75, and 9.71 ksi. Monolithic beam specimens were included to provide a bound on the horizontal shear strength. The combination of variables for each of the 19 specimens is detailed in Table 2.

Table 2: Test Matrix

Beam	Specimen ID	Interface Finish	Loading Method	Interface Width [in.]	Web Steel Area, A_{sweb} [sq.in.]	Flange Strength [ksi]	Effective Prestress [ksi]
1	A4.4	As-Placed	Five-Point	5	0.2	5.67	141.3
2	B4.1	Broom	Five-Point	5	0.2	5.67	142.1
3	M10.1	Monolithic	Five-Point	5	0.0	9.71	139.9
4	R2.1	Rake	Five-Point	5	0.2	3.11	141.5
5	R4.4	Rake	Five-Point	5	0.2	5.67	143.1
6	R10.1	Rake	Five-Point	5	0.0	8.75	140.3
7	Sh4.1	Sheepsfoot	Five-Point	5	0.2	5.67	140.3
8	A4.1	As-Placed	Two-Point	2	0.2	5.67	140.2
9	A4.3	As-Placed	Two-Point	2	0.2	5.67	140.1
10	B4.3	Broom	Two-Point	2	0.2	5.67	140.2
11	M10.2	Monolithic	Two-Point	2	0.0	9.71	140.2
12	M10.3	Monolithic	Two-Point	2	0.0	9.71	140.2
13	R2.2	Rake	Two-Point	2	0.2	3.11	140.2
14	R2.3	Rake	Two-Point	2	0.2	3.11	140.2
15	R4.2	Rake	Two-Point	2	0.2	5.67	140.2
16	R4.3	Rake	Two-Point	2	0.2	5.67	140.2
17	R10.2	Rake	Two-Point	2	0.0	8.75	140.2
18	R10.3	Rake	Two-Point	2	0.0	8.75	140.2
19	S4.2	Smooth	Two-Point	2	0.2	5.67	140.2

Test Setup

Composite beam-flange specimens without ties were tested over a simple span of ten feet. The beams were inverted in a self-reacting test setup for loading and installation convenience. The inversion of the specimens altered the normal force on the interface; however, the change is insignificant compared to the applied load. Equal load was applied at a quasi-static rate to failure through the use of 30 ton jacks serviced by a single hydraulic pump. Two loading configurations were used to investigate the un-reinforced interface behavior: five-point and two-point loading (Figure 3).

In order to examine the service state of horizontal shear stresses, five equally spaced point loads simulated uniform loading of the specimen (Figure 3). As in practice, a uniform load configuration effectively approximates the service demands experienced by a highway bridge girder (i.e. dead-weight, environmental loads, heavy traffic loads, etc). Additionally, the distribution of the point loads through twelve-inch neoprene bearing pads reduced the local normal stress on the interface considerably. Thereby the shear-friction mechanism of the interface was minimized and low bound values for service state horizontal shear stresses were obtained. Although the five-point specimens were loaded to failure, primary observations and measurements were made prior to cracking. In standard practice, cracking at service loads is avoided and the beam is designed to fail in a ductile, flexural failure mode.

The failure state of horizontal shear stress was examined under the two-point loading condition. Point loads placed equidistant from the midspan provided the horizontal shear necessary to fail the specimen in the longitudinal shear mode prior to flexural or shear crack formation. Regions of high horizontal shear at either end of the specimen caused slip to initiate at the tip of the beam-flange interface. The point loads were distributed over a reduced length of 6-in. to minimize the local normal stress on the section.

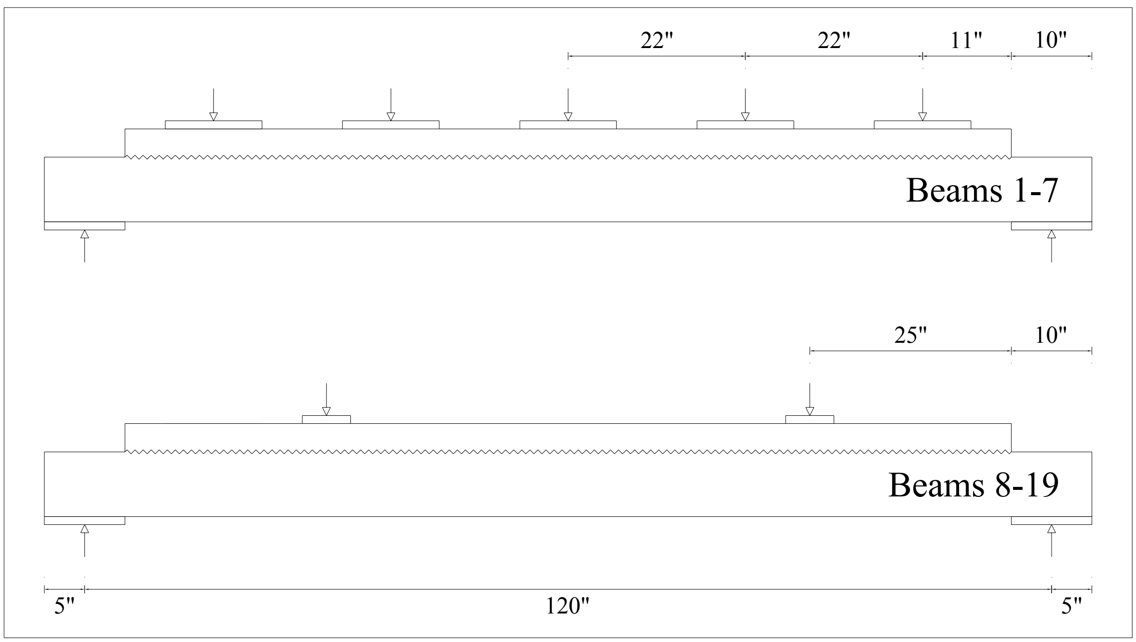

Figure 3: Specimen elevation and loading configurations

Test Specimens

As recognized by Loov and Patnaik, the length of flange within an effective depth of the beam restrains the longitudinal shear failure mode.[16] Therefore, the flange of each specimen was shortened at either end to prevent undesired effects on the horizontal shear behavior. The resulting elevation view is shown in Figure 3. To ensure a horizontal shear failure in the two-point load configuration the interface was reduced by over fifty percent. Based on an initial prestress of 182 ksi and an assumed loss of twenty percent, the five- and two- point specimens were designed to achieve horizontal shear stress levels in excess of 300 and 750 psi, respectively. Web-shear failure was precluded through the use of transverse ties. Flange reinforcement was designed in accordance with PennDOT bridge design code[24]. The section size is on the order of previous horizontal shear studies.[4,10] The cross-section dimensions of the specimens and the reinforcement properties based on mill certifications are shown in Figure 4.

The specimens were fabricated at a local prestressed, precast concrete component manufacturer. All nineteen beams were cast from the same high early strength concrete mix. Mix designs can be found in Table 3, with respective cylinder stress-strain data presented in Figure 5. Special care was then taken in finishing the beam interface before casting the flanges. Transfer of prestress occurred within twenty-four hours of concrete placement. The flanges were cast of three different mixes shortly thereafter.

Table 3: Concrete mix designs and properties

Property	Units	Properties per Cubic Yard			
		9.7ksi Web	3.1ksi Flange	5.7ksi Flange	8.8ksi Flange
Cement Type III	lbs.	556	377	589	558
Coarse Aggregate SSD – Dyer 67	lbs.	1290	1819	1918	1290
MB Glenium 3030 NS HRWR	oz.	84.9	-	-	84.7
Pozzolith 100 XR Retarder	oz.	25.2	-	-	9.6
VR Standard Air Entrainment	oz.	6.9	6.1	5.8	7.0
Design Water / Cement Ratio	-	0.3	0.7	0.5	0.3
Air Content	%	6.1	7.5	5.1	5.3
Slump	in.	5.9	5.0	4.8	5.9

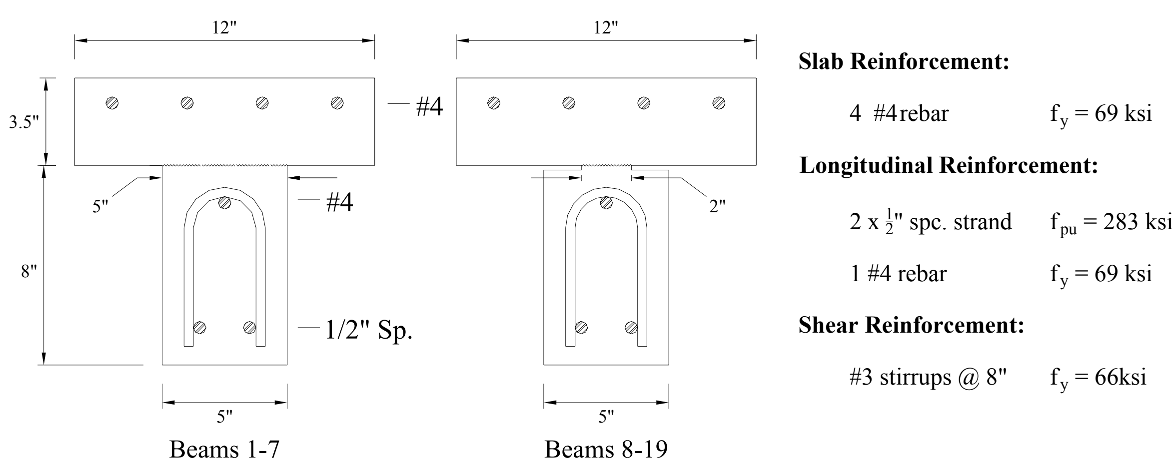

Figure 4: Typical specimen cross-sections

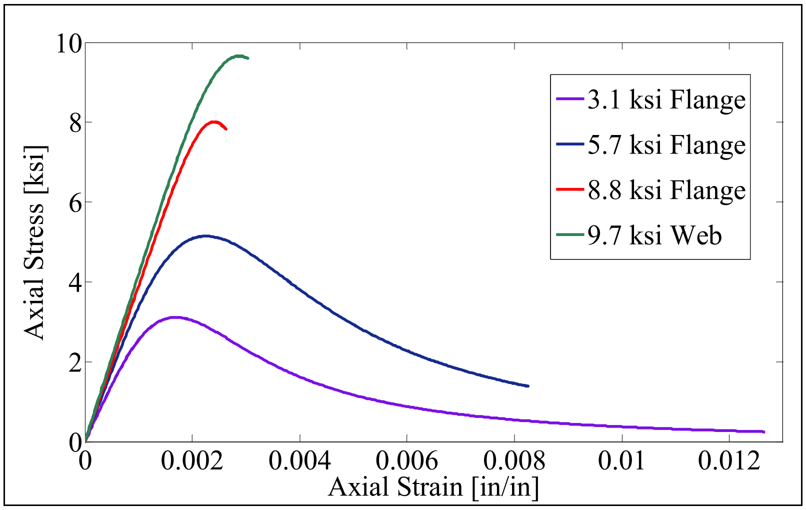

Figure 5: Concrete stress-strain curves

Instrumentation and Horizontal Shear Stress Measurement

Traditional measurements of load and deflection were taken to allow for characterization of the specimen's global behavior. In addition, local measurements of slip and strain permitted close observation of the interface activity (Figure 6). Three to four slip gages were placed in equal intervals along the predicted failure planes and the slip development along the entire interface was monitored. Horizontal shear stress at the interface was measured using two surface mounted strain gages along the flange section depth.

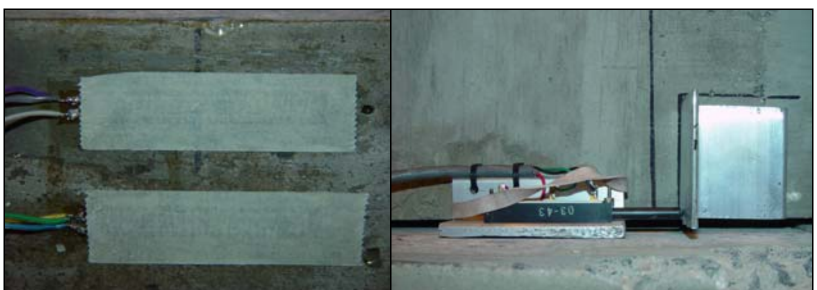

A) Strain Measurement B) Slip Measurement

Figure 6: Instrumentation configurations

The strain profile resulting from the gage measurements was coupled with concrete cylinder stress-strain data to produce a flange stress profile. This stress profile was then integrated over the flange depth and width to obtain the flange force and corresponding horizontal shear stress at the interface. The horizontal shear stress computed using the previously presented methods are illustrated in Figure 7.

Although the analytical results of the AASHTO and elastic methods are nearly indistinguishable, it is not hard to see that they underestimate the horizontal shear stress result provided by the strain data. The integration typically resulted in higher horizontal shear stress, yet the deviation from the AASHTO and elastic methods was never consistent.

Therefore, the following data is based on the elastic method using cracked section properties when the rupture strength of the section is exceeded. This approach yields a conservative, yet realistic (does not over-underestimate, like ACI) estimate of the horizontal shear stress levels.

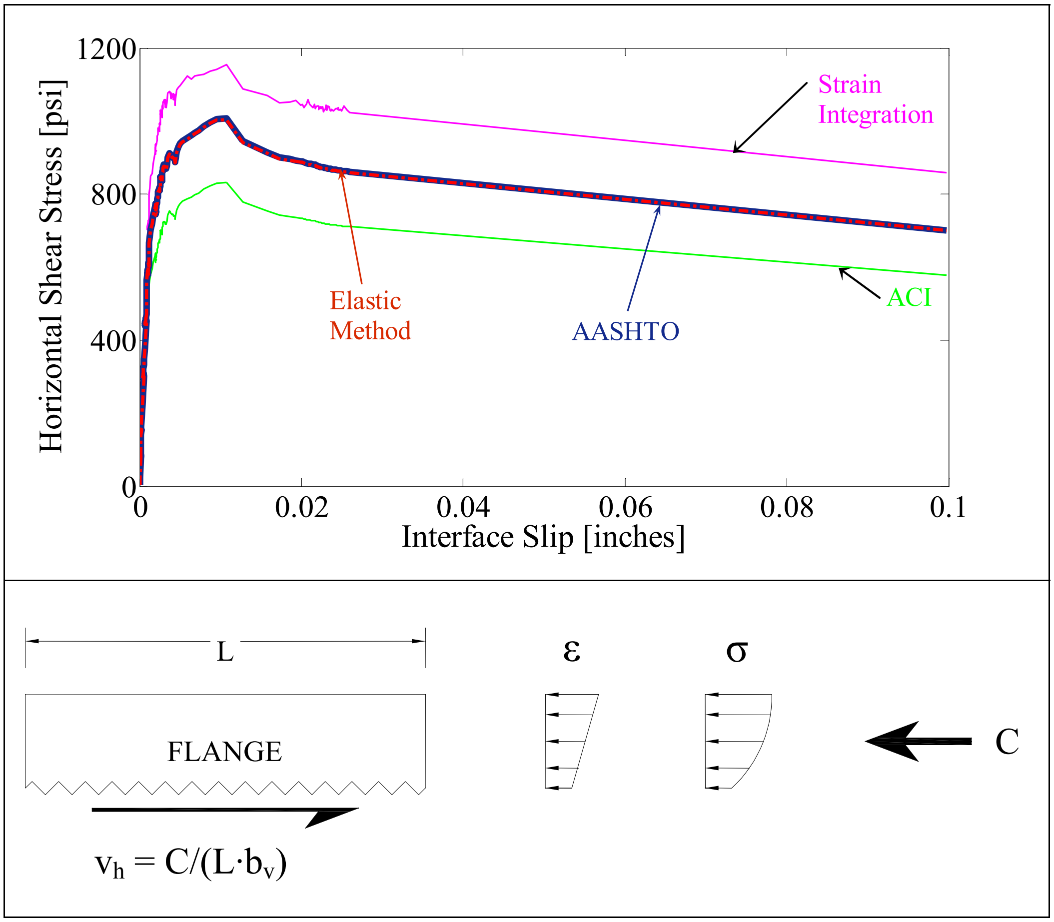

Figure 7: Typical strain profile integration and result [Beam 14, R2.3]

RESULTS AND DISCUSSION

General Behavior of Five-Point Load Specimens

The five-point specimens were loaded incrementally with interface observations made between each step. After a few increments of load, at approximately 28 kips, flexural cracks were observed on tensile face of the beam. As loading continued, flexure-shear cracks extended down into the beam-flange interface, with failure occurring between thirty-five and sixty kips. Failure of the section was generally attributed to the rapid growth of a flexure-shear crack within the outer thirds of the specimen. Nevertheless, pure flexural failure due to fracture of the tensile strands did occur on one occasion (specimen 5, R4.4). Typical five-point failures are shown in Figure 8.

A) Flexural [Beam 5, R4.4] B) Flexure-Shear [Beam 4, R2.1]

Figure 8: Typical five-point failures

No visual observations of interface distress or failure were made during the five-point tests. However, to confirm the monolithic behavior of the section, the load-slip relation was examined. Minute slip increases were measured with rising load. The slip rarely exceeded one-hundredth of an inch at cracking and promptly returned to zero when the specimen was unloaded. This was attributed to compatibility of the interface. Due to the elastic nature of the results, it is believed the interface was maintained throughout the five-point load tests. It also is significant to note that all variations of interface roughness and topping strength delivered an average horizontal shear stress capacity of over 300 psi at service loads (before cracking).

The results for the five-point load tests are presented in Table 4. The specimen, the failure mode and the level of horizontal shear stress at the initiation of flexural cracking are presented.

Table 4: Five-point load results

Beam	Specimen ID	Failure Mode	Failure Load Kips	Horizontal Shear Stress at Cracking psi	Interface Slip at Cracking inches
1	A4.4	Flexure-Shear	44.3	341.1	0.0046
2	B4.1	Flexure-Shear	56.2	341.1	0.0021
3	M10.1	Flexure-Shear	36.6	350.1	0.0035
4	R2.1	Flexure-Shear	45.1	321.6	0.0018
5	R4.4	Flexure	57.2	341.1	0.0028
6	R10.1	Flexure-Shear	53.3	345.6	0.0020
7	Sh4.1	Flexure-Shear	49.0	341.1	0.0365
			Average	340.2	0.0076

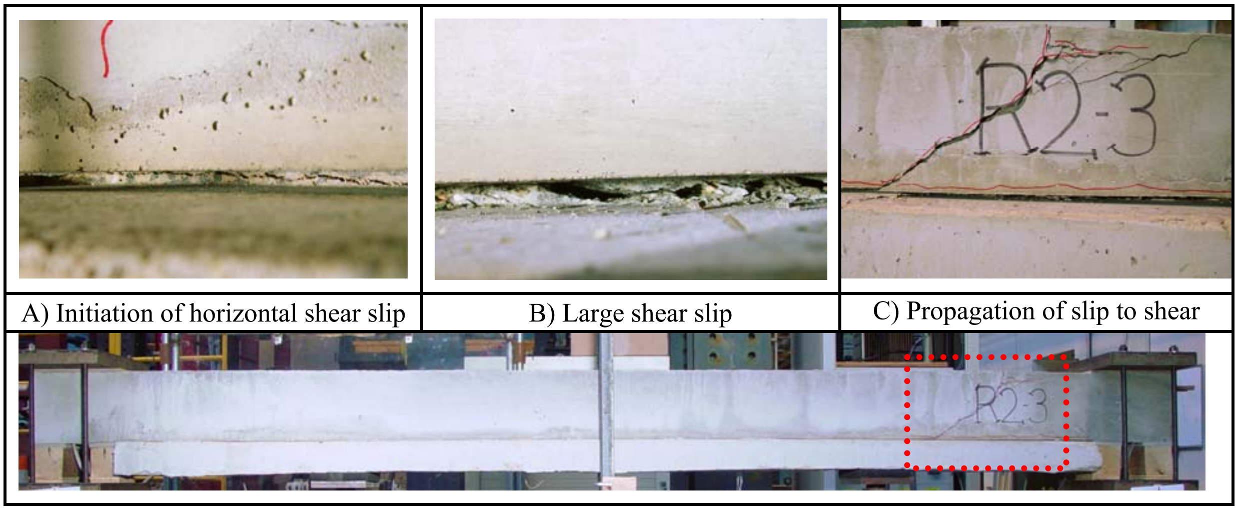

A) Initiation of horizontal shear slip | B) Large shear slip | C) Propagation of slip to shear

Figure 9: Typical failure progression [Beam 14, R2.3]

General Behavior of Two-Point Load Specimens

Loaded in a similar manner, the two-point specimens exhibited subtle signs of impending failure. Applying the initial increments of load led to observations of fine diagonal cracks at the interface. With increased load the interface diagonal cracks connected, forming a continuous separation from the tip of the interface to the respective loading point. For high strength toppings, the longitudinal shear failure that followed was violent, with large translations of the flange and beam. Low strength topping failures were benign in comparison. Regardless of the flange strength, the longitudinal failure was always succeeded by flexure-shear failure due to the reduced section capacity. The photos (Figure 9) and load-slip curve (Figure 10) presented here graphically illustrate the progression of horizontal shear failure observed in the two-point series of testing.

The succession of horizontal shear and flexure-shear failure occurred between twenty-five and forty kips. Corresponding values of horizontal shear stress capacity range from 780 to 1160 psi; where failure horizontal shear stress was recorded at the maximum load. In comparison to a monolithic section, the composite sections achieved 60-90% of full composite action. While the interface may be artificially strengthened by the close proximity of the point loads, the measured capacity is an order of magnitude greater than current design approaches. Two-point series results are tabulated in Table 5.

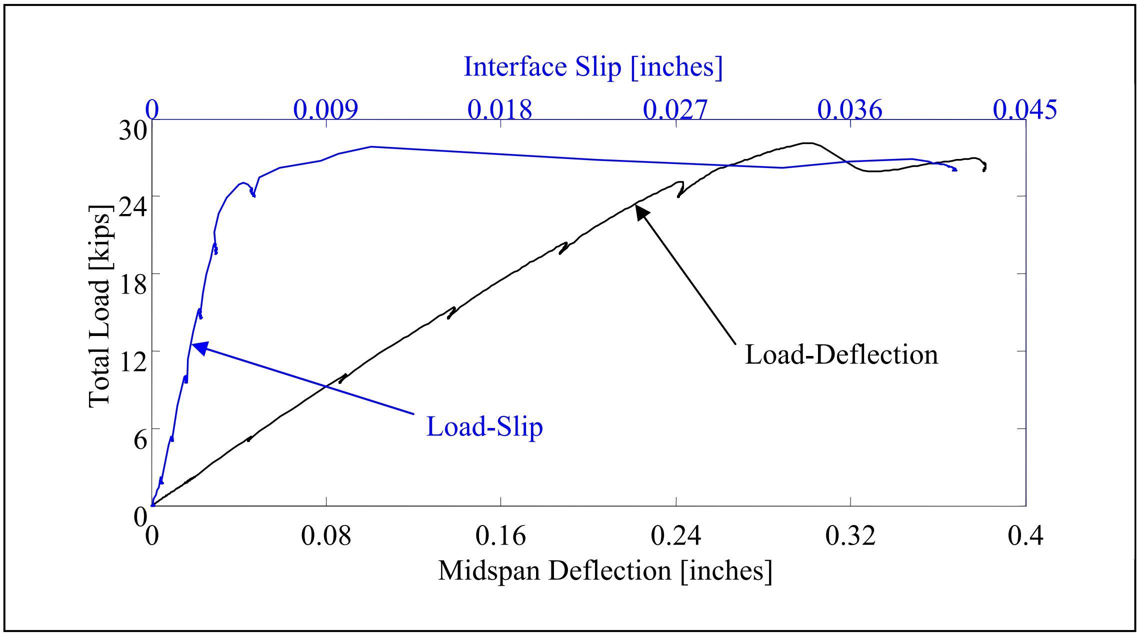

Figure 10: Typical load-slip and load-deflection curve [Beam 13, R2.2]

Table 5: Two-Point Load Results

Beam	Specimen ID	Failure Mode	Failure Load kips	Horizontal Shear Stress at Failure psi	Interface Slip at Failure inches
8	A4.1	Horizontal-Shear	27.9	863.21	0.0281
9	A4.3	Horizontal-Shear	34.4	1060.8	0.0064
10	B4.3	Horizontal-Shear	32.2	993.17	0.0105
11	M10.2	Horizontal-Shear	33.9	1067.0	0.0124
12	M10.3	Flexure-Shear	39.2	1248.1	0.0084
13	R2.2	Horizontal-Shear	28.1	850.13	0.0133
14	R2.3	Horizontal-Shear	33.6	1015.1	0.0114
15	R4.2	Horizontal-Shear	32.4	1001.0	0.0107
16	R4.3	Horizontal-Shear	37.9	1165.9	0.0090
17	R10.2	Horizontal-Shear	37.4	1141.3	0.0121
18	R10.3	Horizontal-Shear	34.9	1073.6	0.0119
19	S4.2	Horizontal-Shear	25.5	787.72	0.0176
			Average	1022.3	0.0127

Horizontal Shear Strength versus Interface Roughness

To examine the effects of interface roughness on horizontal shear capacity, results can be isolated from a series of beams with a common topping strength. The results are presented in Table 6.

Table 6: Capacity versus Interface Roughness

Series -	Interface Finish	Flange Strength ksi	Horizontal Shear Stress at Failure Psi
S4	Smooth	5.67	787.72
A4	As-Placed	5.67	962.01
B4	Broom	5.67	993.17
R4	Rake	5.67	1083.5

Although there is no suitable way to numerically grade the roughness of each finish, the ascending order of the interface strengths was expected. A physical description of the finishes will help to clarify:

1. Smooth: Finish achieved through the use of a magnesium float. No aggregate protrusion.
2. As-Placed: Consolidated with a vibratory probe. Texture slumped out. Little if any aggregate protrusion.
3. Broom: Rough textured finish applied with a coarse bristle broom. No aggregate protrusion.
4. Rake: Very rough textured finish applied with a ¼" tined rake. Little if any aggregate protrusion.

After the two-point tests were complete, the failed interfaces were exposed to gain further insight. Figure 12 and Figure 13 include post-failure photos of the interface finishes. The photos reveal that two separate mechanisms caused the horizontal shear failure. In the case of the weaker interface finishes, the flange and beam sections moved relative to one another without shearing significant amounts of aggregate. In some cases, the original interface finish was clearly distinguishable. In contrast, the rake finish caused the interface to shear in a monolithic mode. The bond was maintained and surrounding aggregate was sheared in the longitudinal failure.

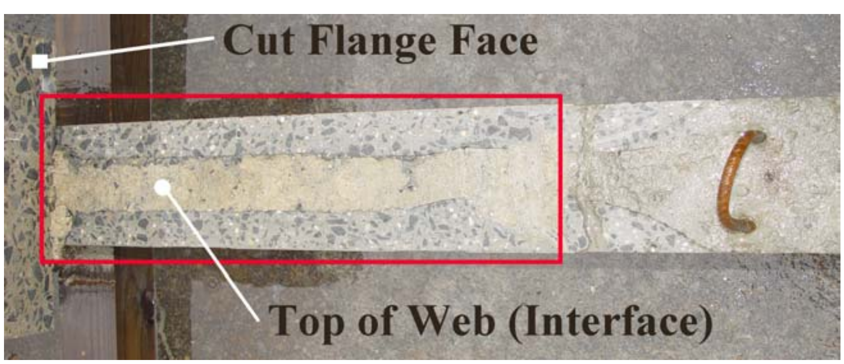

Figure 11: Overall view of failure section with flange removed

a) As-Placed [Beam 9, A4.3]

b) Broom [Beam 10, B4.3]

Figure 12: Gradual slip

a) Monolithic [Beam 12, M10.3]

b) Rake [Beam 16, R4.3]

Figure 13: Brittle fracture

Horizontal Shear Strength Versus Concrete Strength

To examine the effects of concrete strength on horizontal shear capacity, results can be isolated from a series of beams with a common interface finish. The results are presented in Table 7.

Table 7: Capacity versus concrete strength

Series	Interface Finish	Flange Material Strength [ksi]	Horizontal Shear Stress at Failure [psi]
R2	Rake	3.11	932.62
R4	Rake	5.67	1083.5
R10	Rake	8.75	1107.5

Given a high strength concrete beam with three lower strength toppings, the horizontal shear failure will always occur through the flange material. Consequently this research program has succeeded in creating a wide range of topping strengths. Although the corresponding data does not follow a linear trend, it follows the convention that a higher strength flange will yield a greater horizontal shear capacity.

CONCLUSIONS

The horizontal shear capacity of composite concrete beams without ties has been examined for service state and failure load conditions, four levels of interface roughness, and three ratios of slab to beam concrete compressive strength. From the results and discussion presented here, the following conclusions can be made:

1. Horizontal shear stresses, post-processed from strain data, were consistently higher than results provided by the three analytical methods presented. The classical elastic method, coupled with load-appropriate gross and cracked section properties, is recommended for computation of horizontal shear stress levels. Although the elastic method still underestimates the stress levels, it is the least conservative of the three methods.
2. An average horizontal shear stress of *340 psi* was achieved for the service state. This result is more than *three times* the least conservative design estimate for horizontal shear capacity at failure.
3. An average horizontal shear stress of *1022 psi* was achieved for the failure condition. Again, this result is more than *ten times* the least conservative design estimate for horizontal shear capacity at failure.
4. A positive trend is revealed when specimen capacities of the same topping strength, but different interface roughness are compared. That is, horizontal shear strength increases with increasing interface roughness.
5. A similar trend is revealed when specimen capacities of the same interface roughness, but different flange strength are compared. Horizontal shear strength increases with increasing flange strength.
6. The service state and failure load behavior of the ¼” rake finish was very similar to that of the monolithic section. Although a time consuming finish, the rake application is recommended for the best composite performance.

The conclusions and discussion presented indicate that the current recommendations for horizontal shear capacity can be relaxed. However, these results are based on monotonic load applications. To verify the applicability of this study for highway applications, additional tests should be conducted under high cycle demands.

ACKNOWLEDGEMENTS

The project was financed by Schuylkill Products Inc. and a grant from the Commonwealth of Pennsylvania, department of Community and Economic Development, through the Pennsylvania Infrastructure Technology Alliance (PITA) and through the support of, the Pennsylvania Department of Transportation, and the Precast Association of Pennsylvania. The researchers would like to thank Mark Hoover and the staff at Schuylkill Products Inc. for their assistance with fabrication and John Hoffner and the staff at Fritz Laboratory and ATLSS research Center for their assistance with testing.

REFERENCES

1. Revesz, S., "Behavior of Composite T-Beams with Prestressed and Un-prestressed Reinforcement," *ACI Journal*, V. 24, No. 6, Feb. 1953 (Proceedings V.49), pp. 585 – 592.
2. Ozell, A. M., and Cochran, J. W., "Behavior of Composite Lintel Beams in Bending," *PCI Journal*, V. 1, No. 1, May 1956, pp. 38 – 48.
3. Kaar, P. H.; Kriz, L. B.; and Hognestad, E., "Pilot Tests of Continuous Girders," *Journal of the Research and Development Laboratories*, Portland Cement Association, V. 2, No. 2, May 1960, pp. 21 – 37.
4. Hanson, N. W., "Horizontal Shear Connections," *Journal of the Research and Development Laboratories*, Portland Cement Association, V. 2, No. 2, May 1960, pp. 38 – 58.
5. ACI-ASCE Committee 333, "Tentative Recommendations for Design of Composite Beams and Girders, for Buildings," *ACI Journal*, V. 57, No. 6, Dec. 1960, pp. 609 – 628.
6. Mattock, A. H., and Kaar, P. H., "Precast-Prestressed Concrete Bridges, 4 – Shear Tests of Continuous Girders," *Journal of the Research and Development Laboratories*, Portland Cement Association, V. 3, No. 1, Jan. 1961, pp. 47 – 56.
7. Grossfield, B., and Birnstiel, C., "Tests of T-Beams with Precast Webs and Cast-in-Place Flanges," *ACI Journal*, *Proceedings* V. 59, No. 6, June 1962, pp. 843 – 851.
8. Saemann, J. C., and Washa, G. W., "Horizontal Shear Connections Between Precast Beams and Cast-in-Place Slabs," *ACI Journal*, Vol. 61, No. 11, November 1964, pp. 1383 – 1409.
9. Bryson, J. O.; Skoda, L. G.; and Watstein, D., "Flexural Behavior of Prestressed Split-Beam Composite Concrete Sections," *PCI Journal*, Vol. 10, No. 3, June 1965, pp. 77 – 91.
10. Evans, R. H., and Chung, H. W., "Horizontal Shear Failure of Prestressed Composite T-Beams with Cast-in-Situ Lightweight Concrete Deck," *Concrete*, April 1969, pp. 124 – 126.
11. Bryson, J. O., and Carpenter, E. F., "Flexural Behavior of Prestressed Concrete Composite Tee Beams," National Bureau of Standards, Building Science Series 31, July 1970.
12. Concrete Technology Associates (CTA), "Composite Systems without Roughness," Technical Bulletin 74-B6, June 1974.
13. Concrete Technology Associates (CTA), "Composite Systems without Ties," Technical Bulletin 76-B4, April 1976.
14. Barnoff, R. M.; Orndorff, J. A., Jr.; Harbaugh, R. B., Jr.; and Rainey, D. E., "Full Scale Test of a Prestressed Bridge With Precast Deck Planks," *PCI Journal*, V. 22, No. 5, September – October 1977, pp. 67 – 83.
15. Seible, F., and Latham, C. T., "Horizontal Load Transfer in Structural Concrete Bridge Deck Overlays," *Journal of Structural Engineering*, ASCE, V. 116, No. 10, October 1990, pp. 2691 – 2710.

16. Loov, R. E., and Patnaik, A. K., “Horizontal Shear Strength of Composite Concrete Beams with a Rough Interface,” *PCI Journal*, V. 39, No. 1, January – February 1994, pp. 48 – 69.
17. Kumar, N. V., and Ramirez, J. A., “Interface Horizontal Shear Strength in Composite Decks with Precast Concrete Panels,” PCI Journal, V. 41, No. 2, March – April 1996, pp. 42 – 55.
18. Tan, K. H.; Guan, L. W.; Lu, X.; and Lim, T. Y, “Horizontal Shear Strength of Indirectly Loaded Composite Concrete Beams,” *ACI Structural Journal*, V. 96, No. 4, July – August 1999, pp. 533 – 539.
19. Patnaik, A.K., “Longitudinal Shear Strength of Composite Concrete Beams with a Rough Interface and no Ties,” *Australian Journal of Structural Engineering*, V. SE1, No. 3, 1999, pp. 157-166.
20. Patnaik, A. K., “Behavior of Composite Concrete Beams with Smooth Interface,” *Journal of Structural Engineering*, V. 20, No. 10, April 2001, pp. 881 – 900.
21. Gohnert, M., “Horizontal Shear Transfer Across a Roughened Surface,” *Cement & Concrete Composites*, V. 25, No. 3, April 2003, pp 379 – 385.
22. ACI 318-05, *Building Code Requirements for Structural Concrete and Commentary*. American Concrete Institute, 2005.
23. AASHTO, “LRFD Bridge Design Specifications,” Third Edition, 2006 Interim Revisions, American Association of State Highway and Transportation Officials, Washington, DC, 2006.
24. Commonwealth of Pennsylvania Department of Transportation, “Design Manual Part 4,” Publication 15M, Harrisburg, PA, 2000.